

Stefan problem and beyond

B.F. Kostenko, J. Pribiš, I.V. Puzynin

Joint Institute for Nuclear Research, Dubna

141980 Moscow region, Russia

Abstract

We claim that the celebrated Stefan condition on the moving interphase, accepted in mathematical physics, can not be imposed if energy sources are spatially distributed in the volume. A method based on Tikhonov and Samarskii ideas for numerical solution of the problem is developed. Mathematical modelling of energy relaxation of some processes useful in modern ion beam technologies is fulfilled. Necessity of taking into account effects completely outside the Stefan formulation is demonstrated.

Keywords: Mathematical simulation; heat transfer; phase transition

The address for correspondence:

Dr. B.F. Kostenko
Laboratory of Information Technologies
Joint Institute for Nuclear Research
141980, Dubna, Moscow region
Russia

E-mail: kostenko@jinr.ru

Tel.: +007-096-21-64-069; fax: +007-096-21-65-145

1 Introduction

The Stefan problem concerns solid-liquid or liquid-vapor phase transitions when moving **unknown beforehand** surface S of phase transition is formed (see, e.g., [1]). In fact, a formulation of the Stefan problem was given for the first time by G. Lamé and B.P. Clapeyron in 1831 for a particular case of equal temperature of liquid and crystalline phases [2]. In 1889 J. Stefan published four papers devoted to the subject (in particular, to the description of soil freezing) in which the problem was formulated in a general form [3]. According to it, for the interphase the following condition

$$K_{sol} \frac{\partial T(x_S + 0, t)}{\partial x} - K_{liq} \frac{\partial T(x_S - 0, t)}{\partial x} = L \rho_{sol} V_S, \quad (1)$$

defining Stefan's problem, has been suggested. Here $V_S = d\xi_S/dt$ is the velocity of the boundary surface S , K_{sol} and K_{liq} are thermal conductivities of material for solid and liquid phases, L and ρ_{sol} are the melting heat and density, correspondingly. Condition (1) has a clear physical meaning. Indeed, according to the Fourier law, heat flow \mathbf{j} is proportional to the temperature gradient,

$$\mathbf{j} = -K \mathit{grad} T.$$

Therefore, the left-hand side of (1) is the heat absorbed in the unit of area per the unit of time. The expression in the right-hand side is the heat connected with freezing or melting of material crossed per the unit of time by the the unit of area.

A complete mathematical formulation of the Stefan problem includes, besides (1), a condition of continuity on the surface S separating solid and liquid phases

$$T|_S = T^*, \quad (2)$$

where T^* denotes temperature of the phase transition, and the energy conservation law

$$\rho C \frac{\partial T}{\partial t} = -\mathit{div} \mathbf{j} + q(\mathbf{x}, t).$$

Here $q(\mathbf{x}, t)$ represents the power of external heat sources, C is the specific heat. In the original Stefan papers $q(\mathbf{x}, t) \equiv 0$, so that the whole heat transfer has been considered to be a consequence of the temperature gradient inside the medium.

If one also specifies initial and boundary conditions, the Stefan problem can be solved more often approximately, but sometimes exactly. Particular examples of suitable boundary conditions are considered below.

Relations (1) and (2) are usually used in numerical algorithms explicitly. Another approach was suggested by A.N. Tikhonov and A.A. Samarskii in 1953 [4]. According to it, conditions (1) and (2) are included themselves into the energy conservation equation to obtain generalized formulation of the Stefan problem in the form

$$(\rho C + L \delta(T - T^*)) \left(\frac{\partial T}{\partial t} + \mathbf{v} \mathit{grad} T \right) = \mathit{div}(K \mathit{grad} T) + q(\mathbf{x}, t), \quad (3)$$

where the term $L \delta(T - T^*) \partial T/\partial t$ describes the additional heat input expended on the phase transformation, $\mathbf{v} \mathit{grad} T$ takes into account possible temperature change due to

convection (hereafter we ignore it for simplicity). The main idea of this approach is quite clear, too. Namely, it is suggested to treat the heat of fusion L as an additional component of the thermal capacity ρC which gives contribution only at the point of phase transition.

Lately Samarskii and his followers have turned this idea into effective numerical algorithms (see, e.g. [5]). But even in those papers equation (3) is considered only as a corollary of the condition (1). For example, it was derived in [1] by substituting expression $L \delta(T - T^*) \partial T / \partial t$ instead of the term $L \delta(x - \xi_S(t)) V_S$, which is assumed to be included in the heat equation to account for the heat absorption on 2-dimensional interface S .

The purpose of this paper is to show that the condition (3) supplies us with a more powerful description of phase transitions, that may be used even in the case when (1) and (2) are not applicable.

2 Heuristic arguments

As it was mention above, the possibility of solving the classical Stefan problem by making use of condition (3) has been demonstrated by Samarskii and his co-authors. Therefore, we only consider an example when (3) is applicable and (1), (2) are not. To this end let us study the following problem:

$$(\rho C + L \delta(T - T^*)) \frac{\partial T}{\partial t} \operatorname{div}(k \operatorname{grad} T) + q(t), \quad (4)$$

$$T(\mathbf{x}, 0) = T_0 < T^*,$$

where all parameters of (4) are suggested to be independent of \mathbf{x} . Due to the spatial uniformity, it is evident that the condition

$$\operatorname{grad} T = 0$$

holds on the solutions of (4). In this case Eq. (4) is reduced to an ordinary differential one

$$(\rho C + L \delta(T - T^*)) \frac{dT}{dt} = q(t) \quad (5)$$

with the initial condition

$$T(0) = T_0.$$

Integrating both sides of (5) over t just near the phase transition temperature T^* , one obtains

$$\int_{T^*-0}^{T^*+0} (\rho C + L \delta(T - T^*)) dT = \int_t^{t+\delta t} q(t) dt, \quad (6)$$

where δt is a time necessary for the phase transition. It is evident from (6) that

$$\delta t \geq \frac{L}{Q}, \quad (7)$$

where Q is the maximum value of $q(t)$ in the interval $(t, t + \delta t)$. The inequality (7) means that the phase transition at a fixed spatial point lasts **a finite, distinct from zero, time**.

This simple example shows something completely different from the Stefan description of the phase transition. Let us examine it carefully.

1. First of all, instead of gradual warming (or cooling) up the pattern due to the influence of one of its boundaries, here we have an uniformly heated layer. Therefore, creation of 2-D surface $S(y, z)$ separating the solid and liquid phases in x is evidently impossible due to a total equivalence of all spatial points x .
2. One can also expect that finiteness of the phase transition time, δt , forces all points within **a spatial layer of nonzero thickness** to be at the same temperature T^* . This is expected even in the case when the power deposition $q(x, t)$, unlike in the example considered, is spatially irregular¹.

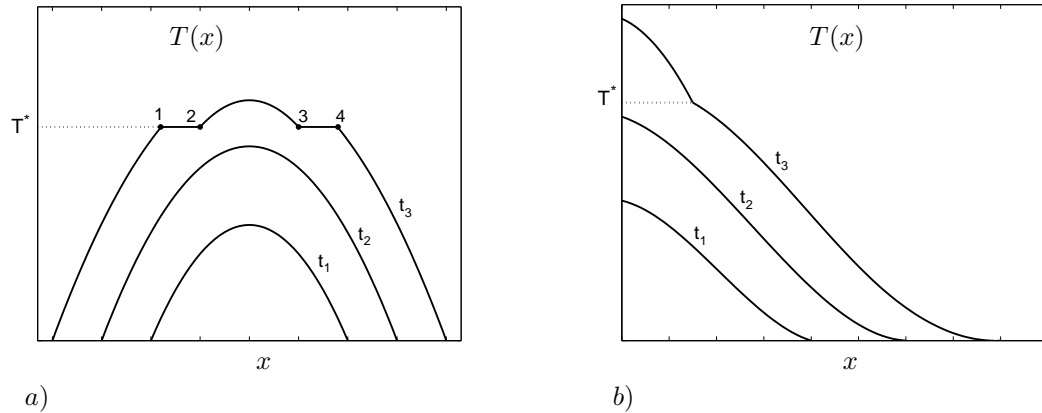


Fig. 1. Evolution of the temperature distribution in the pattern for: a) a case of spatially distributed sources of heat, b) the classical Stefan problem (with heating from left to right). Here $t_1 < t_2 < t_3$.

If we consider δ -function in (3) as a limit of a bounded function $D(T - T^*)$ localized in the vicinity of $T = T^*$, then the possibility to obtain the solution shown in Fig. 1(a), or analytically,

$$\frac{\partial T}{\partial t} \rightarrow 0, \quad \text{grad } T \rightarrow 0,$$

follows from the indefiniteness

$$D(T - T^*) \frac{\partial T}{\partial t} \rightarrow \infty \cdot 0,$$

springing up in the left-hand side of (3). Clearly, that this indefiniteness can take a finite value and compensate in a space region with nonzero thickness the spatially distributed source $q(\mathbf{x}, t)$ which contributes to the right-hand side of (3). This, of course, is no more true if the external sources are absent and heat enters the pattern only through its boundary.

¹Indeed, let material has just reached the temperature T^* at some point \mathbf{x} and now begins receiving its portion of the heat necessary for melting. Then another adjacent point $\mathbf{x} + \Delta\mathbf{x}$, which attained the melting temperature merely a little earlier, can be still in the state of heat receiving and, therefore, must have **the same temperature T^*** (see Fig.1).

In a general case, one can expect existence of **two jumps** for spatial derivatives of temperature on the boundaries S of the **volume** V_{T^*} with $T = T^*$, instead of one for the classical Stefan problem, but the condition (1) is hardly met for any of them (see Fig. 1(a), where intersection of the boundary S by (x,y)-plane in points 1, 2, 3 and 4 is seen). Indeed, to prove the existence of two jumps — one from the side of the solid and another from the side of the melted phase — it is sufficient only to show that the spatial derivative on the surface S , **taken externally**, is not equal to zero. The co-ordinates of the boundary $\vec{\xi}(t)$ can be found as a solution of an equation

$$T(\mathbf{x}, t) - T^* = 0,$$

where $T(\mathbf{x}, t)$ is the solution of the heat equation (3) outside the volume V_{T^*} . Taking the total temporal derivative, one obtains

$$\frac{\partial T}{\partial t} + \text{grad } T \cdot \frac{d\vec{\xi}}{dt} = 0.$$

Thus $\text{grad } T = 0$ automatically implies $\partial T / \partial t = 0$. It is evident that such conditions are impossible if the external sources are not adjusted specially to stabilize the temperature in the infinitesimal layers adjacent to the volume V_{T^*} just before and just after the phase transition.

3 Beam induced phase transitions

To verify the conclusions which we have just come to, let us study **numerically** the dynamics of phase transition induced by a short powerful ion beam in solids. At present this technology is really used for modification of surface layers to create new materials with unique physical and chemical properties (see, e.g. [6]). The process is underlain by the equation for heat transfer which we discussed in the previous sections:

$$\rho(T)c(T)\frac{\partial T}{\partial t} = \frac{\partial}{\partial x} \left(k(T)\frac{\partial T}{\partial x} \right) + q. \quad (8)$$

The initial and boundary conditions could be taken in the form:

$$T(x, 0) = T_0, \quad \frac{\partial T(0, t)}{\partial x} = \frac{\partial T(l_0, t)}{\partial x} = 0.$$

Let us consider, for definiteness, an iron pattern, which thermal properties are described in popular reference books, and choose dimensionless (**DL** for brevity) variables

$$T := T/T_0, \quad x := x/l_0, \quad t := t/\tau$$

as follows:

$$\begin{aligned} T_0 &= 293 \text{ K}, & l_0 &= 10^{-5} \text{ m (the pattern thickness),} \\ \tau &= 3 \cdot 10^{-7} \text{ s (duration of ion beam pulse from an accelerator).} \end{aligned}$$

For DL power deposition q we take a simple model, shown in Fig. 2 and 3,

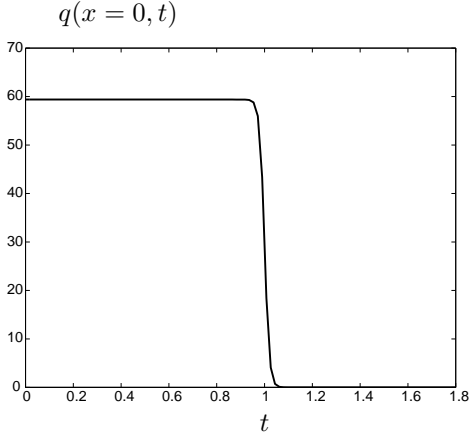


Fig. 2. Power deposition: t -dependence

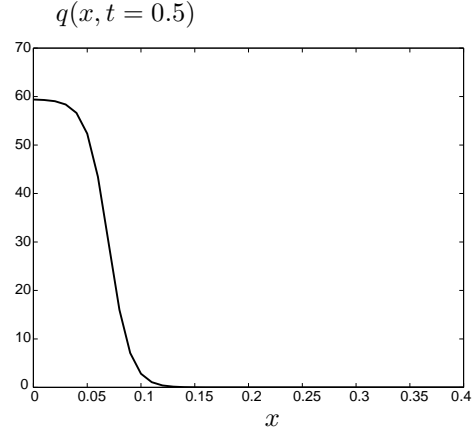


Fig. 3. Power deposition: x -dependence

with analytical representation

$$q(x, t) = Q q_1(x)q_2(t),$$

where

$$q_i(z) = \frac{1}{1 + \exp \mu_i(z - z_i)}$$

and Q describe the total DL energy brought into the pattern (here $Q = 59.44$, $x_1 = 0.07$, $t_1 = 1$, $\mu_i = 100$). For simplicity, we neglect in (8) a small difference between physical parameters for the solid and liquid phases.

Now, using of the general idea due to Tikhonov and Samarskii [4], we assume an expression:

$$\rho(T)c(T) = 1 + \lambda\delta(T - T^*, \Delta)$$

for DL specific heat, where λ denotes the DL heat of fusion and $\delta(T - T^*, \Delta)$ is an approximate δ -function, smoothed with the help of the Gaussian distribution of width Δ (see Fig. 4)².

Now Eq. (8) can be solved numerically on the space-time grid x and t with steps h_x and h_t , within intervals $x \in (0, 1)$, $t \in (0, t_{max})$:

$$x_j = h_x \cdot j, \quad j = 0, \dots, n_x, \quad h_x = 1/n_x,$$

$$t_k = h_t \cdot k, \quad k = 0, \dots, n_t, \quad h_t = t_{max}/n_t,$$

where n_x and n_t are numbers of partitions.

²There were other methods of smoothing in original papers by Samarskii et al. They used regularization on the space grid.

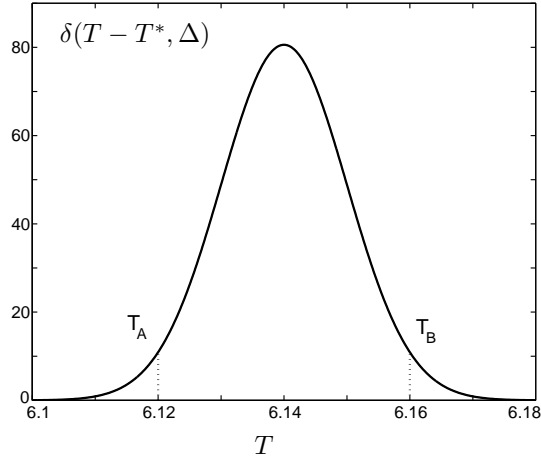


Fig. 4. Approximate δ -function with maximum at T^* and smearing equals Δ (for $\Delta = 0,03$)

The following difference scheme with weights γ was implemented (see [7] for details):

$$e_j^k \frac{T_j^{k+1} - T_j^k}{h_t} = k_0 \left[\gamma \frac{T_{j+1}^{k+1} - 2T_j^{k+1} + T_{j-1}^{k+1}}{h_x^2} + (1 - \gamma) \frac{T_{j+1}^k - 2T_j^k + T_{j-1}^k}{h_x^2} \right] + q_j^{k+\frac{1}{2}}, \quad (9)$$

where

$$T_j^k = T(x_j, t_k), \quad e_j^k = \rho(T_j^k)c(T_j^k), \quad q_j^{k+\frac{1}{2}} = q(x_j, t_k + \frac{h_t}{2}),$$

and the upper index numerates different moments of time (time “levels”), the lower one specifies a set of spatial co-ordinates. The scheme is absolutely convergent at $\gamma = 0.5$ and possesses the second-order accuracy for both variables.

From initial condition $T(x, 0) = T_0$, values T_j^0 ($j = 0, \dots, n_x$) on a zero time level are known. The boundary conditions

$$\frac{T_1^k - T_{-1}^k}{2h_x} = \frac{T_{n_x+1}^k - T_{n_x-1}^k}{2h_x} = 0, \quad k = 1, \dots, n_t$$

allow one to introduce symmetric points $x_{-1} = -h_x$ and $x_{n_x+1} = 1 + h_x$ with appropriate values $T_{-1}^k = T_1^k$ and $T_{n_x+1}^k = T_{n_x-1}^k$ respectively. So, we can use the Eq. (9) in points x_0 and x_{n_x} . Using initial and boundary conditions, we obtain a system of n_x linear algebraical equations with the same number of variables. Thus, under the accepted approximation, we reduced the partial differential equation (8) to system (9) of linear algebraic equations. The matrix of this system is tridiagonal and after its solution³ we obtain value T_j^1 ($j = 0, \dots, n_x$) at the first time level. Repeating this process, values T_j^k on every time level k are computed.

The result of straightforward verification of the Stefan condition (1) is shown in Fig. 5, where the function

$$\phi(t) = k \left(\left. \frac{\partial T}{\partial x} \right|_{T_A} - \left. \frac{\partial T}{\partial x} \right|_{T_B} \right) - \lambda \frac{d\xi}{dt} \quad (10)$$

³Recursive relations for determining the solution of algebraic problem (9) comprise the well-known sweep method, called also forward-backward or Thomas algorithm [1].

is depicted.

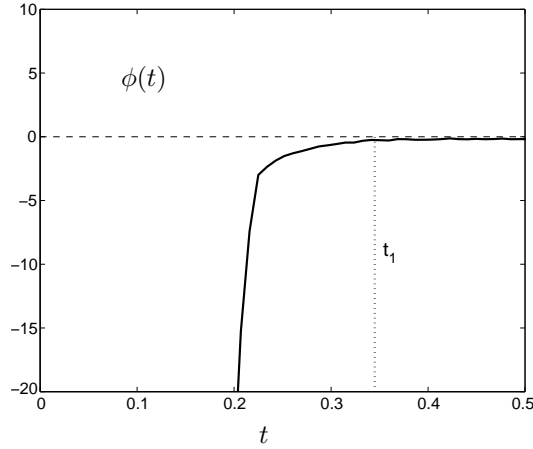


Fig. 5.

The left and right points, in which the spatial derivatives of temperature were taken in (10), are shown in Fig. 4. They define a spatial layer which nearly the whole fusion energy is absorbed within. From Fig. 5 one can see that condition (1) is satisfied indeed, but only **after a characteristic relaxation time t_1 has elapsed**. The physical meaning of t_1 is clear from Fig. 6. Namely, it corresponds to the transition from a rapid to slow motion of the exterior interphase surface. In the case when boundary motion is rapid, the heat necessary for fusion is brought into the melting layer **directly from the external source $q(x, t)$** . The slow motion corresponds to the ordinary Stefan mode when the process is controlled mainly by the heat entered into the layer through its boundary.

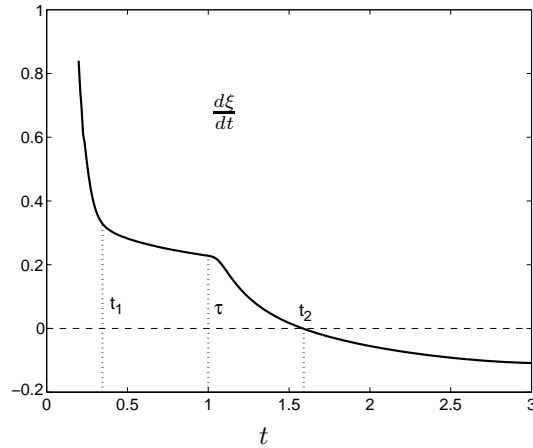


Fig. 6. Velocity of the boundary surface

It is also seen from Fig. 6 that transition to the Stefan mode takes place earlier than the external source to be totally turned off:

$$t_1 < \tau.$$

Time t_2 shown in Fig. 6 denotes a moment when the thickness of the melted material begins to diminish due to heat escape into a more cooler solid phase.

Fig. 7 and 8 also confirm the conclusions which we have come to in the previous section. Formation of the “tableland” (whose height corresponds to the fusion temperature) for spatial temperature distribution is distinctly seen in Fig. 7. The narrow strip restricted by two dashed lines in Figs. 7 and 8 exhibits the width of the smoothed δ -function. We believe that existence of **two** breaks for the spatial derivative is masked in Fig. 7 with this δ -function smearing. Fig. 8 demonstrates a temperature evolution for two divorced spatial points. One can make sure that the above mentioned time interval corresponding to the **same temperature** at the **different spatial points** really exists. It is evident that such a behavior of temperature has nothing to do with the traditional description in the framework of (1) and (2).

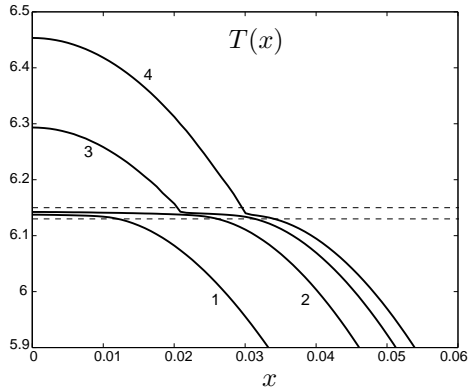


Fig. 7. Spatial temperature distribution for: 1) $t = 0,162$; 2) $t = 0,186$; 3) $t = 0,204$; 4) $t = 0,216$ ($\Delta = 0,01$)

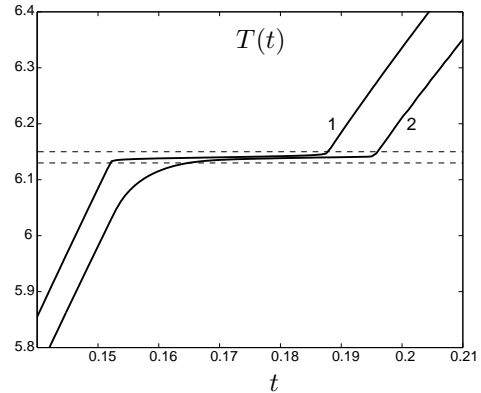


Fig. 8. Evolution of temperature for: 1) $x = 0$; 2) $x = 0,04$ ($\Delta = 0,01$)

Fig. 9 shows a time-dependence of the interphase coordinate. Numbers 1 and 2 denote the regions where verification of the Stefan condition (1) is impossible due to **Δ -instability**. It means that small variations of fusion temperature value, T^* , lead to a drastic change of interphase position (see dotted lines in Fig. 9).

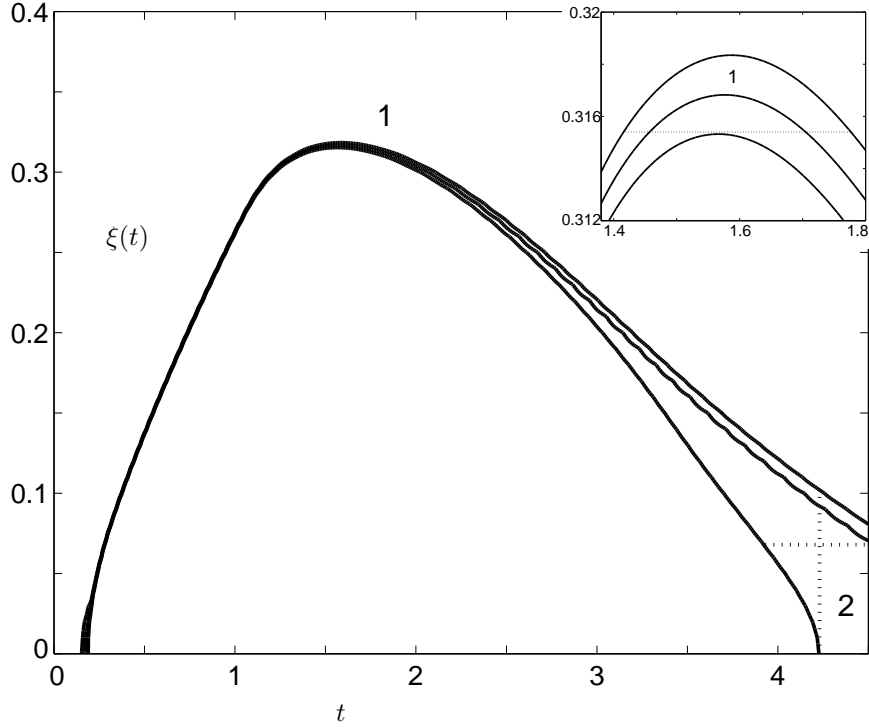


Fig. 9. Time dependence of the interphase coordinate. Here a curve in the middle corresponds to the fusion temperature equals T^* . For the upper and lower curves, the fusion temperature is chosen to be at $T^* - \Delta/2$ and $T^* + \Delta/2$, accordingly ($\Delta = 0,01$)

4 Track formation in solids

The next example demonstrating the preference for the δ -function approach is connected with the problem of track formation in solids. In fact, at present nobody knows with certainty the main mechanism responsible for these processes. Furthermore, it seems like the universal model explaining all of them does not exist and different materials behave differently under heavy ion attack. Here we assume the so-called thermal spike model based on the following system of two coupled nonlinear differential equations (see, e.g. [8] and references therein):

$$\rho C_e(T_e) \frac{\partial T_e}{\partial t} = \frac{1}{r} \frac{\partial}{\partial r} \left[r K_e(T_e) \frac{\partial T_e}{\partial r} \right] - g \cdot (T_e - T_i) + q(r, t), \quad (11)$$

$$\rho C_i(T_i) \frac{\partial T_i}{\partial t} = \frac{1}{r} \frac{\partial}{\partial r} \left[r K_i(T_i) \frac{\partial T_i}{\partial r} \right] + g \cdot (T_e - T_i), \quad (12)$$

where T_e and T_i are electrons and lattice temperatures, respectively, C_e, C_i and K_e, K_i specific heat and thermal conductivity for the electronic system and lattice, ρ is the material

density, g the electron-atom coupling, $q(r, t)$ the power brought on the electronic system, r the radius in cylindrical geometry with the ion path as the axis. One can see that electrons receive their energy directly from the external source $q(r, t)$ which takes into account ion energy loss in electron gas. The characteristic duration of source activity is usually in the range $10^{-15} - 5 \times 10^{-15}$ s. According to (12), atoms are heated due to electron-atom coupling represented by the term $g \cdot (T_e - T_i)$. Nuclear interaction of atoms with the projectile ion is relatively small and, therefore, can be neglected. It is clear that coupling is the most effective at the beginning of the relaxation process when $T_e \gg T_i$ and $g \cdot (T_e - T_i) \simeq gT_e$.

The initial conditions can be chosen in a form

$$T_e(r, 0) = T_i(r, 0) = T_0,$$

and the boundary ones⁴ can be taken as

$$\left(\frac{\partial T_e}{\partial r}\right)_{r=0} = \left(\frac{\partial T_i}{\partial r}\right)_{r=0} = 0, \quad T_e(r_{max}, t) = T_i(r_{max}, t) = T_0,$$

where r_{max} was taken of order 10^{-5} cm.

The thermal spike model explains track formation as a structural transition of lattice due to its warming-up and melting with subsequent quenching. These processes are usually accompanied with disorder creation in the lattice. Indeed, rapid quenching leads to a ‘‘conservation’’ of atoms’ random places that were in the melted material just before cooling. For amorphous materials, which are characterized by high disorder of atoms’ positions and small values of thermal conductivity, quenching, quite the contrary, leads to putting atoms’ places in order. But in either case, structural modifications are observed in the microscope as an ion trace in solid.

Besides thermal spike, one may assume the ion spike as well, when the track is formed due to the electrostatic repulsion of ionized atoms. The main reason justifying our utilization of system (11), (12) is an agreement of nuclear track radii, calculated in this framework, with the experimental data [8]. The total formulation of the model includes many physical details, such as a description of the source $q(x, t)$, and is outside the scope of this publication. Here we only touch some problems concerning the main topic of the paper.

A numerical algorithm similar to that described above has been elaborated for numerical solving system (11), (12). The radial distribution of the lattice temperature T_i around the path of **Pb** in amorphous **Ge** at kinetic energy of impinging ions of about 110 MeV is shown in Fig. 10 (for two different moments of time). One can see the typical ‘‘tablelands’’ similar to those discussed in the previous chapter and which could not be obtained in frames of the classical Stefan approach. Our calculations show that the ‘‘tableland’’ exists here only during a transitory time t_1 , when the material is under a strong exposure of the source $g \cdot (T_e - T_i) \simeq g T_e$. It is shorter than $\tau = \varrho C_e / g \approx 10^{-12}$ s (see Fig. 10), where τ is electron-atom relaxation time⁵, characterizing duration of source activity in (12) (compare this conclusion with data presented in Fig. 6).

⁴One should take into account that there is no heat transfer at the center of track.

⁵The formula for τ estimation follows from Eq. (11).

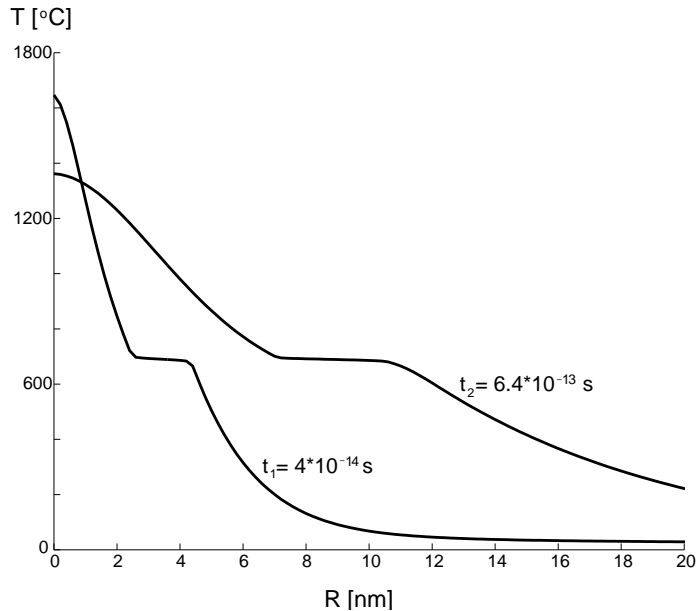


Fig. 10. The radial distribution of the lattice temperature T_i for two different moments of time

It is interesting to note that there is a real, met in the nature, “regularization” of δ -function analogous to that implemented in this paper. For materials with a complex molecular structure (high temperature superconductors, biological molecules, alloys etc.), the melting temperature is not fixed but, instead, smeared within a characteristic interval where atom bonds of different type are gradually destroyed with temperature increase. In this case the only possible approach to the problem should be based on the condition (3). An approximate δ -function, analogous to that shown in Fig. 4, can be extracted here directly from the experiment. In [9], a model based on the smeared δ -function approach and Eqs. (11), (12) was used for computation of effective electron-atom relaxation time τ in a high temperature superconductor. The established τ turned out to be in a good agreement with experimentally observed values.

5 Conclusion

To the best of our knowledge, the peculiarities of phase transition dynamics, we discussed in this paper, have never been considered explicitly in mathematical physics. This fact may be explained partially by the necessity to use **very powerful** spatially distributed external sources of heat, in order the above mentioned effects to be urgent. Such sources were hardly available for industrial applications not long ago. However, the examples which given above are likely evidences of the fact that such sources, “interfering” in the thermal conductive processes, are integral parts of **all** most recent ion beam technologies. The numerical investigations, which have been undertaken, show that the δ -function approach to phase transitions is a suitable instrument to tackle these problems, though the authors of this idea have never used it in such a context.

Within networks of scientific papers devoted to the interphase motion problem, one can

distinguish in retrospect the following logical order: formulation of the Stefan problem (Lame and Clapeiron; Stefan) \longrightarrow application of the δ -function approach for equivalent representation of it (Tikhonov and Samarskii) \longrightarrow numerical implementations of the idea (Samarskii with co-authors; this review) \longrightarrow description of materials with interval distributed fusion temperature (a natural physical interpretation of the previous step). Here we have shown that it is more expedient to **turn over** this order and take its last element as the basis for solving both the classical Stefan problem and a more general one including spatially distributed sources. In other words, both of these solutions could be considered as an idealized limiting case $\Delta \rightarrow 0$ of a natural physical point of view that none of phase transitions take place at the **exactly** defined value of fusion temperature. A peculiarity of a new, found in this paper, solution to Eq. (3) is its “tableland” behavior seen in Figs. 1(a), 7, 8 and 10. Such solutions could never be obtained in the framework of the classical Stefan formulation (compare with Fig. 1(b)).

We would like to express our gratitude to professor M. Toulemonde from CIRIL (Caen) for interest and useful discussion. The authors are grateful to doctors E. Airjan, I. Amirkhanov, I.N. Goncharov and T.P. Puzynina from JINR (Dubna) for stimulating discussions.

This investigation has been supported in part by the Russian Foundation for Basic Research, project No. 02-01-00606.

References

- [1] A.A. Samarskii, P.N. Vabishchevich, *Computational Heat Transfer, Mathematical Modelling*, V.1, p. 30–33 (John Wiley & Sons, Chichester – New-York, 1995).
- [2] G. Lame, B.P. Clapeiron, Ann. de Chem. et de Phys. **XLVII**, 250–256 (1831).
- [3] J. Stefan, Sitzber. Wien. Akad. Mat. naturw. **98**, 473–484, 616–634, 965–983, 1418–1442 (1889).
- [4] A.N. Tikhonov, A.A.Samarskii, *Equations of Mathematical Physics*, p. 266 (GITTL, Moscow, 1953)(in Russian).
- [5] A.A. Samarskii, B.D. Moiseenko, Russian Journ. of Comp. Math. and Math. Phys. **5**, 816–827 (1965).
- [6] G.A. Bleikher, V.P. Krivobokov, O.V. Pashchenko, *Heat and Mass Transfer in Solids under Influence of Powerful Charged Particle Beams* (Nauka, Novosibirsk, 1999) (in Russian).
- [7] N.N. Kalitkin, *Numerical Methods*, pp. 368–371 (M., Nauka, 1978) (in Russian).
- [8] M. Toulemonde, C. Dufour, E. Paumier, Phys. Rev. **B46**, 14362 – 14369 (1992-II).
- [9] I.N. Goncharov, B.F. Kostenko, V.P. Philinova, Phys. Lett. **A288/2**, 111-114 (2001).